CHAPTER IV
RESULTS AND DISCUSSION

4.1 Water Content Analysis

Zeolites usually contain moisture due to its affinity towards water; therefore they must be preheated before use. In order to identify preheating temperature and moisture content, Thermogravimetric analysis was performed.

TGA results (Figure 4.1) shows weight loss with increased temperature as curves immediately decrease when temperature reaches around 50°C and becomes constant at around 350°C. Therefore, water content in zeolites was removed by preheating in an oven with constant heating rate of 10°C from room temperature to 350°C and holding at the temperature for 3 hrs (Table 4.1 shows moisture content in zeolites). In case of CMG273, which is found very sensitive to moisture (due to presence of CuS) and was kept in an evacuated desiccator, the TGA results shows loss of adsorbent material at temperature higher than 100°C with no potential gain (about 1.0% moisture removal only). Therefore, CMG 273 was used directly without any preheating.

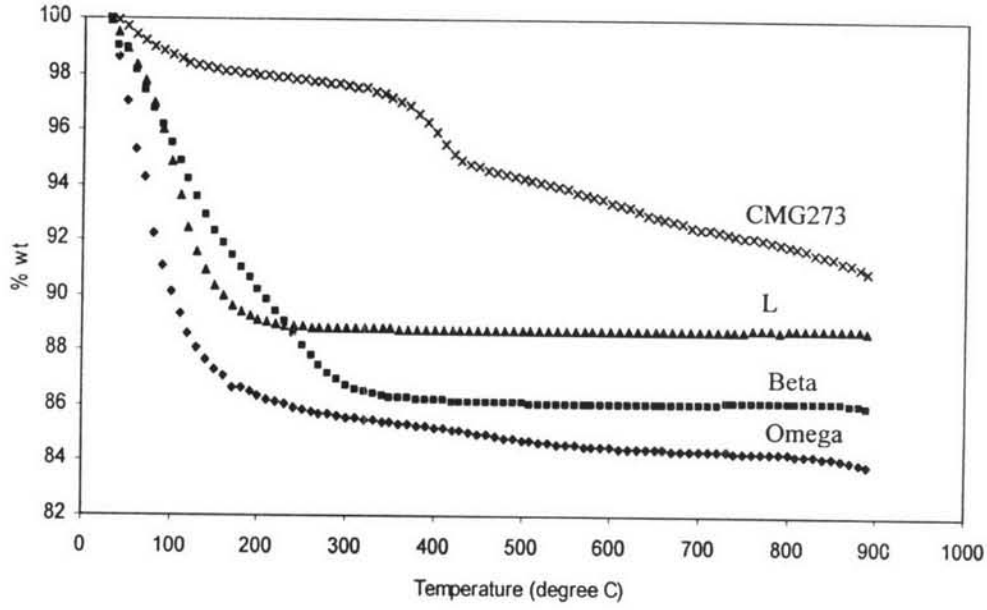

Figure 4.1 Thermograms of zeolites Omega, Beta, L and CMG273.

Table 4.1 Moisture contents in adsorbents

Adsorbent	Moisture Content (%)
Zeolite X	22.5*
Zeolite Y	21.2*
Zeolite L	12.4
Zeolite Beta	16.2
zeolite Omega	13.9

*information obtained from previous work Taechawattanapanich, S. (2004).

The amount of water adsorbed on zeolites X and zeolites Y was found highest (22.5 % for NaX, 21.2 % for NaY). This may be due to the difference in Si/Al ratio (1.3 for NaX, 2.8 for NaY), the higher polarity of NaX results in higher adsorption of water molecules. While lesser moisture content was seen for zeolites omega, beta and L (13.9 % for omega, 16.2 % for beta, 12.4 % for L). A high Si/Al ratio (=8.3) decreases the polarity for zeolite beta. However, zeolite Omega and L have almost same Si/Al ratio (=2.4 and 2.8) as NaY though different levels of moisture have been seen due to much less surface area for zeolite L (300 m^2/g) as compared to NaX (680 m^2/g) and NaY (650 m^2/g) and beta (660 m^2/g). For zeolite Omega one dimension framework reduced the moisture content in it which is further confirmed by looking zeolite L which also have single dimension framework. The single dimension of zeolite reduces the accessibility of moisture from different directions.

4.2 Stability of Metallic Mercury in Container

Metallic mercury is reported very unsuitable for plastic containers (Bouyssiere *et al.*, 2000; Bloom, 2000; Parker *et al.*, 2004; Yan *et al.*, 2003). More than 50% loss of metallic mercury was seen due to adsorption on polypropylene container. Most of the literature recommends the use of glass containers. The statement was also verified through experiments. Figure 4.2 shows only 3% loss of mercury during storage of seven concentrations, varying from 200 to 900 ppb,in a 10 ml glass vial for 3 days while concentrations were measured at the end of each day.

The loss in mercury concentration may be due to volatility of both metallic mercury and n-heptane. The rate of evaporation of n heptane/mercury depends upon frequent openings of container, duration of opening and room temperature as solubility of mercury strongly depends on temperature (Lawrence *et al.*, 1987). At lower temperature solubility decreases rapidly and this is why mercury solutions were kept in a water bath maintained at 30°C. The concentration was measured each time before starting experiment in order to avoid error due to storage.

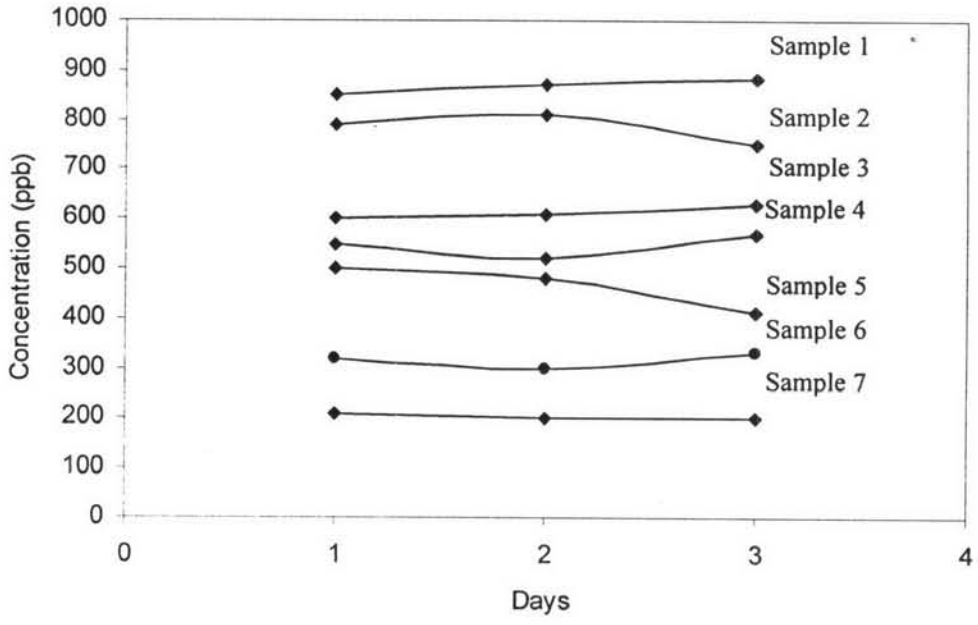

Figure 4.2 Variation in concentration during storage of mercury samples of concentrations (1) 850 ppb, (2) 800 ppb, (3) 600 ppb, (4) 550 ppb, (5) 500 ppb, (6) 300 ppb and (7) 200 ppb.

4.3 Kinetic Study of Metallic Mercury

The adsorption kinetics of metallic mercury on zeolite X and Y is shown in Figure 4.3 and 4.4 (Appendix A1 and A2). The rate of mercury removal is rapid on the initial contact and slows down as the contact time increases. It almost reaches equilibrium in around 100 min. Very similar trends and adsorption capacities have been seen due to similar structure and physical properties for both zeolites X and Y. At lower concentrations of mercury, 20% removal was achieved while at higher concentrations adsorption capacity increased to 30%. The increased adsorption with

increased concentration and lower temperature indicates physical adsorption for both zolites. However, for NaX initial adsorption is slower as compared to NaY. This may be due to higher polarity of NaX (Si/Al= 1.3) than NaY (Si/Al= 2.8) for non polar molecule of metallic mercury.

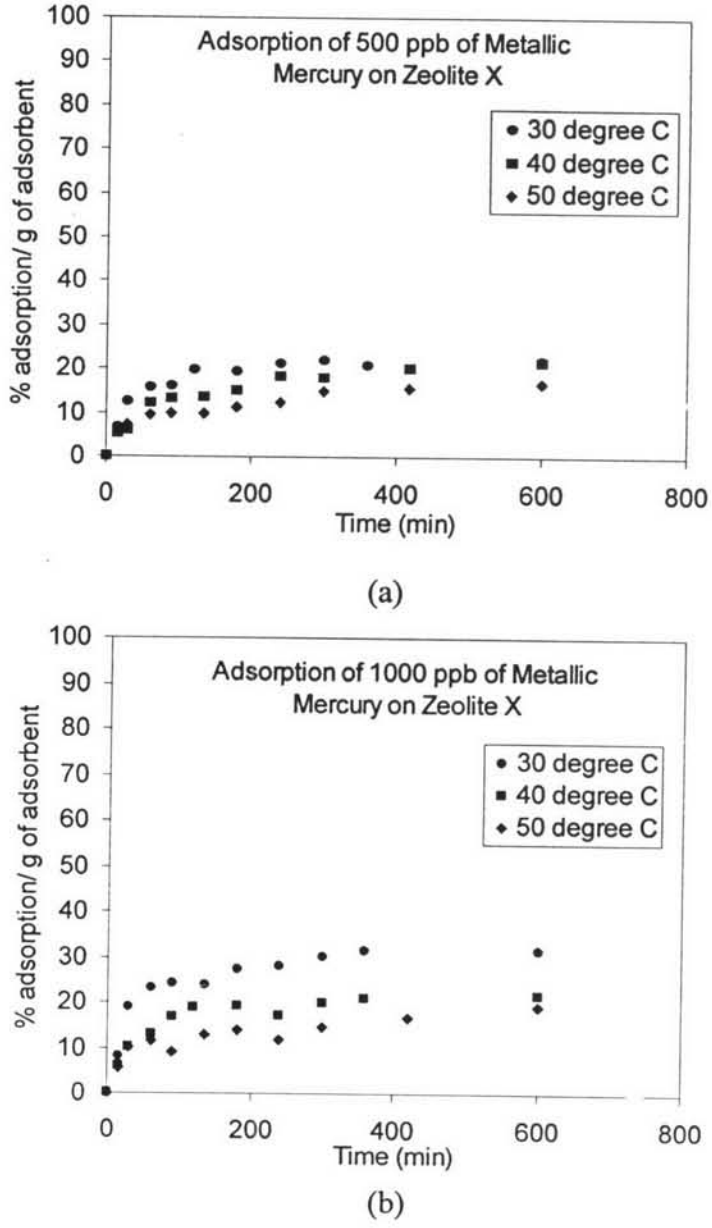

Figure 4.3 Kinetics study of metallic mercury adsorption on zeolite X, for concentrations (a) 500 ppb and (b) 1000 ppb, at 30°C, 40°C and 50°C.

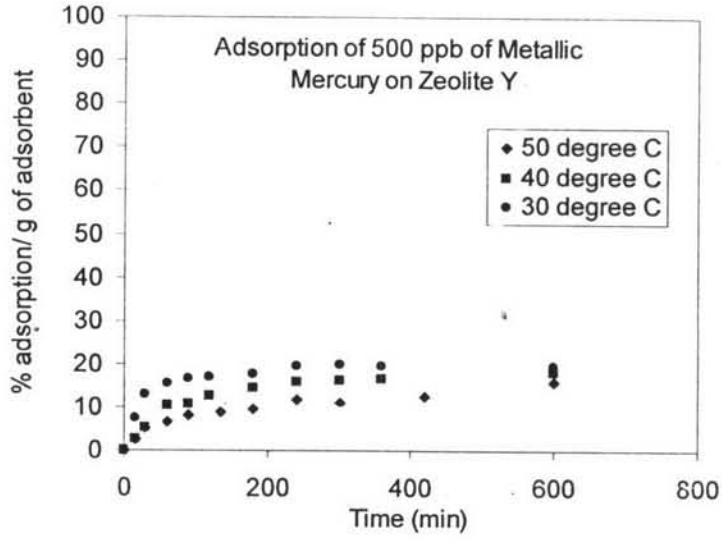

(a)

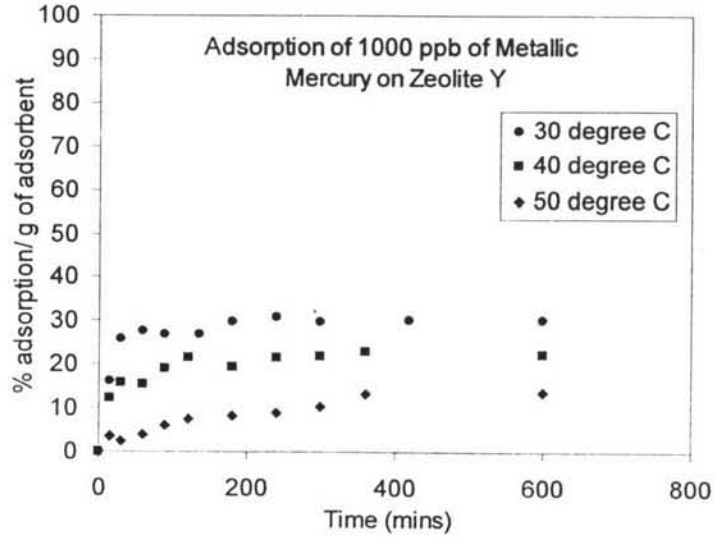

(b)

Figure 4.4 Kinetics study of metallic mercury adsorption on zeolite Y, for concentrations (a) 500 and (b) 1000 ppb, at of 30°C, 40°C and 50°C.

The adsorption of metallic mercury on CMG 273 (Figure 4.5, Appendix A3) was found very fast and mcre than 95% removal was achieved. The adsorption kinetics varied very little with different temperatures. However, capacity was slightly high at higher temperatures. The high removal is due to the active element (CuS on alumina). The adsorption not only increased at higher temperature but also increased

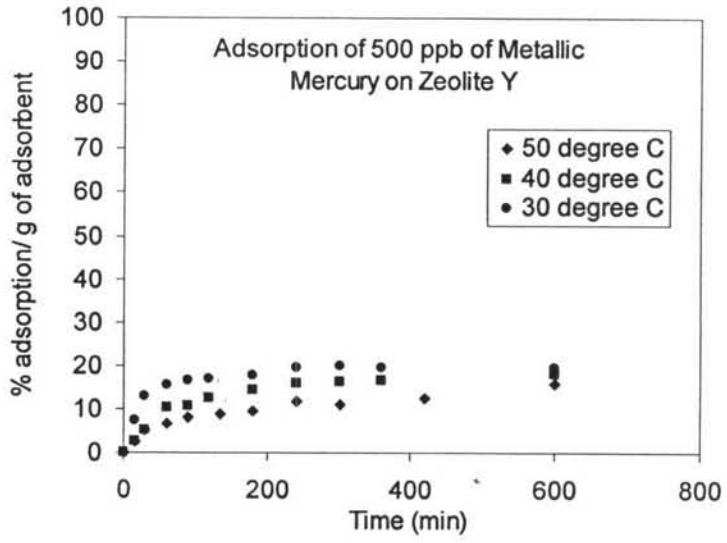

(a)

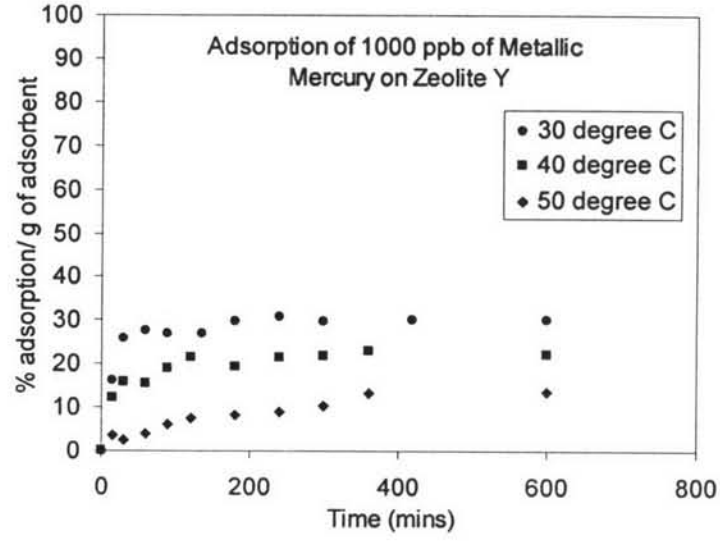

(b)

Figure 4.4 Kinetics study of metallic mercury adsorption on zeolite Y, for concentrations (a) 500 and (b) 1000 ppb, at of 30°C, 40°C and 50°C.

The adsorption of metallic mercury on CMG 273 (Figure 4.5, Appendix A3) was found very fast and more than 95% removal was achieved. The adsorption kinetics was varied very little with different temperatures. However, capacity is slightly high at higher temperatures. The high removal is due to the active element (CuS on alumina). The adsorption is not only increased at higher temperature but

also increased with high concentration. It suggests that, there was physical adsorption also along with chemisorption.

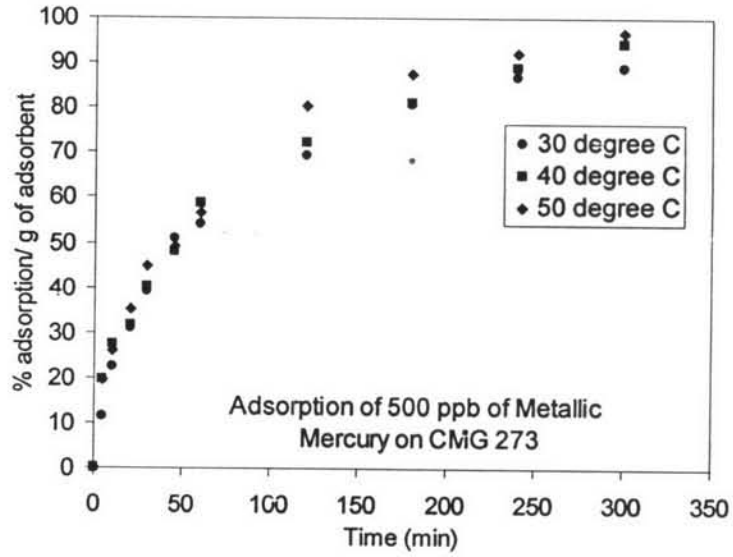

(a)

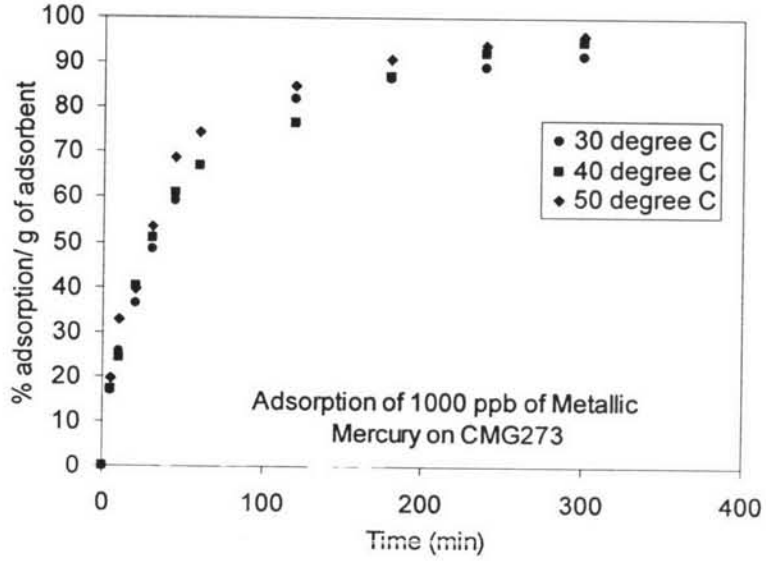

(b)

Figure 4.5 Kinetics study of metallic mercury adsorption on CMG273, for concentrations (a) 500 and (b) 1000 ppb, at 30°C, 40°C and 50°C.

Figure 4.6 (Appendix A4, A5 and A5) shows adsorption kinetics of metallic mercury on zeolites Omega, Beta & L and only 15% average adsorption could be achieved for zeolites Omega and Beta while it was even 10% for zeolite L. Also, there was 10% average fluctuations were found in measurements. Figure 4.7 shows 10% average losses in mercury concentration in all experimental conditions. In addition, trace impurities present in zeolites may also some mercury trap. So, it can be said that the amount of removal may not come from adsorption but only losses and uncertainties.

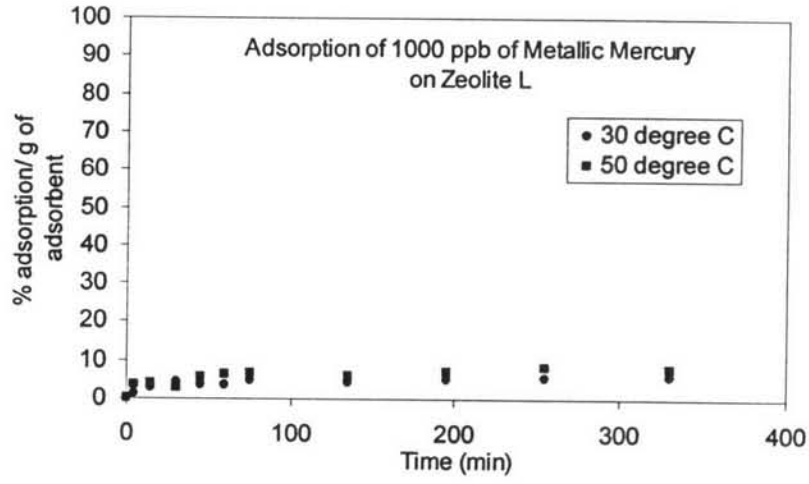

(a)

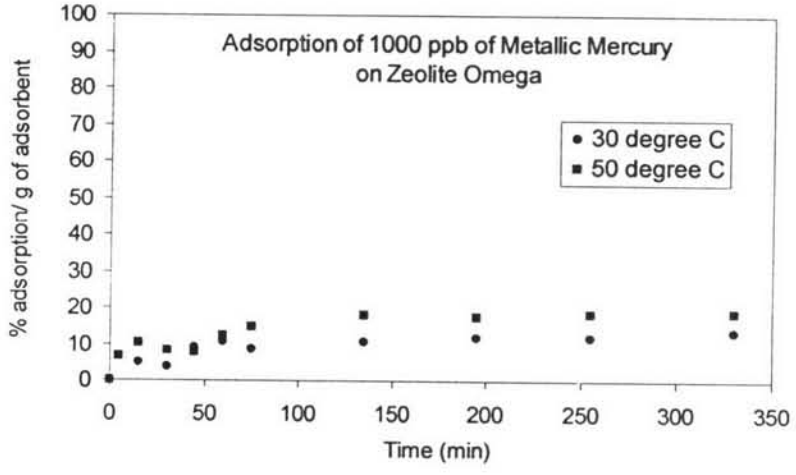

(b)

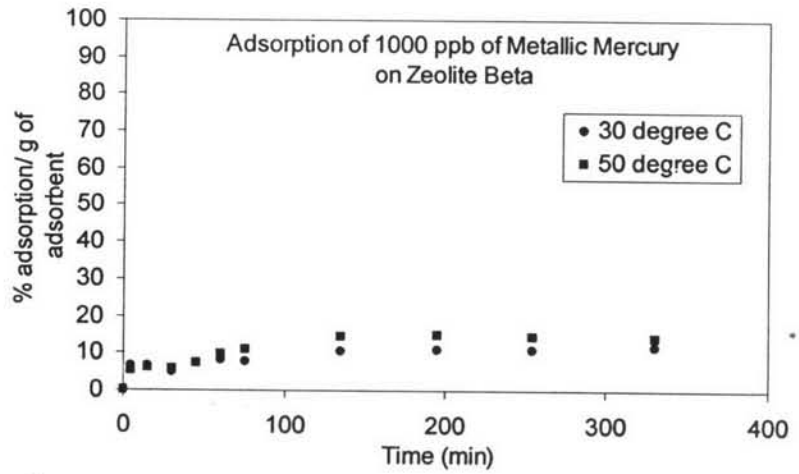

(c)

Figure 4.6 Kinetics study of 1000 ppb of metallic mercury adsorption on zeolites (a) L, (b) Omega and (c) Beta, at 30°C, 40°C and 50°C.

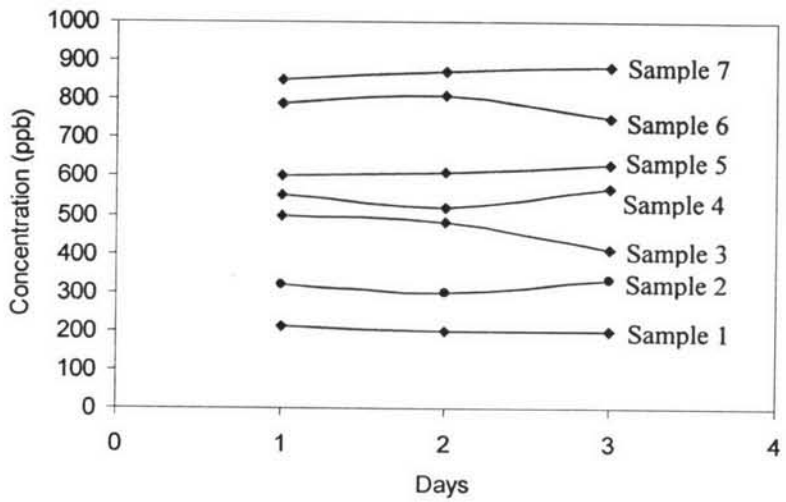

Figure 4.7 Average losses and analytical uncertainties in metallic mercury determination during sampling of (1) 880 ppb, (2) 990 ppb and (3) 890 ppb at 30°C.

There may be two reasons which cause very little adsorption of metallic mercury on zeolites as; the pore openings and compatibility of Hg^{o} with zeolite. All the zeolites used in the experiments have very high polarity due to low Si/Al ratio which makes them unsuitable for non polar molecule of mercury. Also, size of

mercury molecule is very small (3A°) as compared to pore openings (7.4A°). So, mercury atoms can pass through easily without having any interaction.

However, only zeolites NaX and NaY have shown some adsorption while no adsorption was observed for zeolites omega, beta and L. This may be explained on the basis of structure of zeolites. NaX and NaY have cage structures (Figure 2.2) with small openings but big space inside. So, there may be some possibility of mercury storage into cages without having any physical or chemical bond but only due to electronic structure of zeolite. However this is not the case for zeolites omega, beta and L which have straight channel structure (Figure 2.3) having same big opening throughout the length of pore leaving no space for storage.

4.4 Adsorption Isotherms for Adsorbents

The adsorption isotherms for zeolites X, Y, L, Omega, Beta were constructed at temperatures 30°C, 40°C and 50°C. Temperatures higher than 50°C were not selected due to volatility of metallic mercury. Langmuir model is used to explain the adsorption isotherms.

The Langmuir model hypothesizes that there is only one kind of adsorption sites and adsorption energy is same for all adsorption sites. Each site is equivalent to another that can adsorb only one molecule on one distinct adsorption site. The model determines the fraction or the ratio of the number of adsorbed molecules on the total number of molecules required for a complete monolayer, defined as θ (quantity of molecules adsorbed on the solid called q (mol/g of adsorbent). At equilibrium, the adsorption rate (R_{ad}) and desorption rate (R_{de}) are equal:

$$R_{ad} = K_A(1-\theta)C.L \qquad (4.1)$$

$$R_{de} = k_D\theta.L \qquad (4.2)$$

where C is equilibrium concentration of metal mercury, L is total site for a complete monolayer, k_A and k_D are the adsorption and desorption constants respectively. Therefore previous equations can be rearranged as:

$$\theta = q/q_{max} = \frac{bC}{1+bC} \tag{4.3}$$

Thus, the equation can be rearranged to satisfy the first order linear relationship as;

$$\frac{1}{q} = \frac{1}{q_{max}} + \left(\frac{1}{b.q_{max}}\right)\frac{1}{C} \tag{4.4}$$

where b equilibrium constant ($=k_A/k_D$) and q_{max} is maximum quantity adsorbed on solid phase.

Figure 4.8 shows fitting of experimental data (Appendix B1, B2 and B3) for zeolites X, Y and CMG273 into equation 4.4 as below; however, kinetics studies indicates no adsorption on zeolites Omega, Beta and L and for the reason is not plotted.

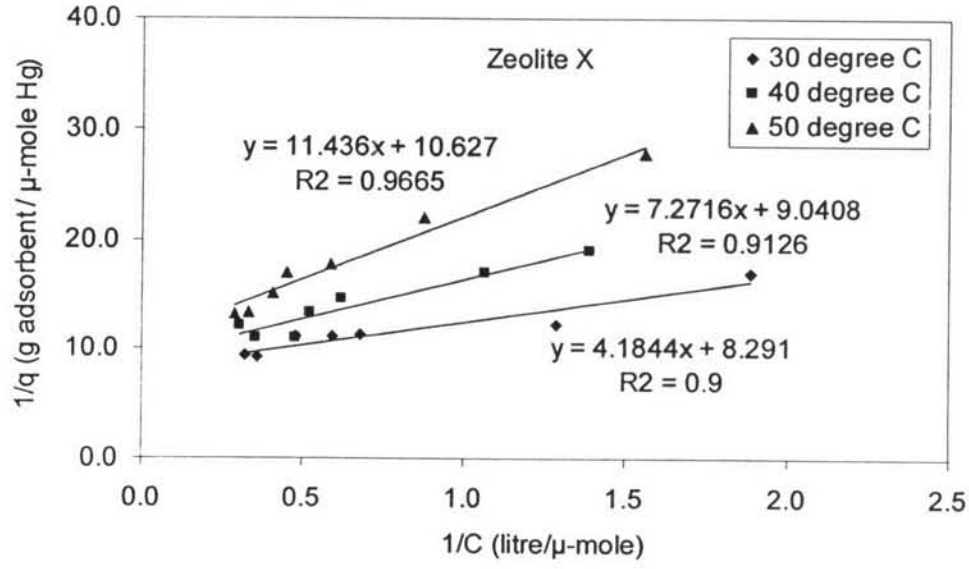

(a)

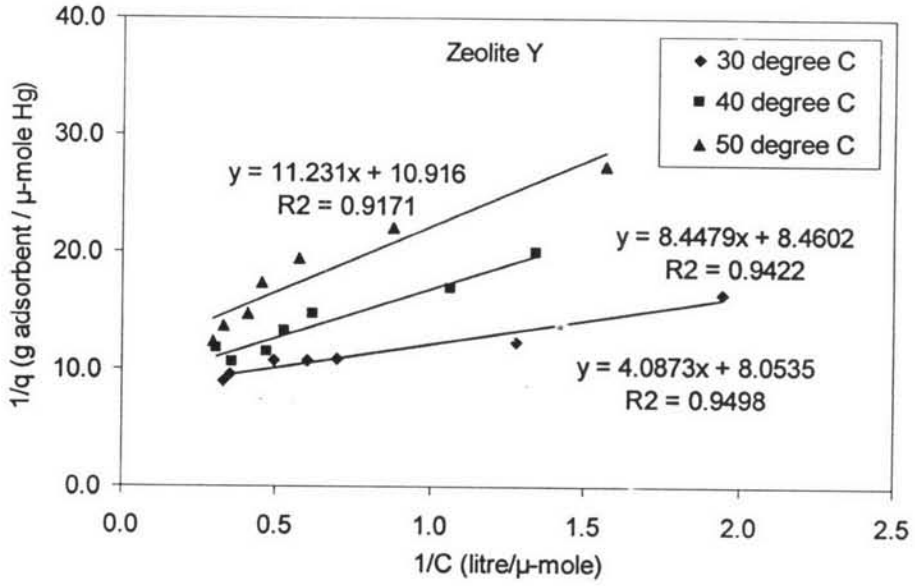

(b)

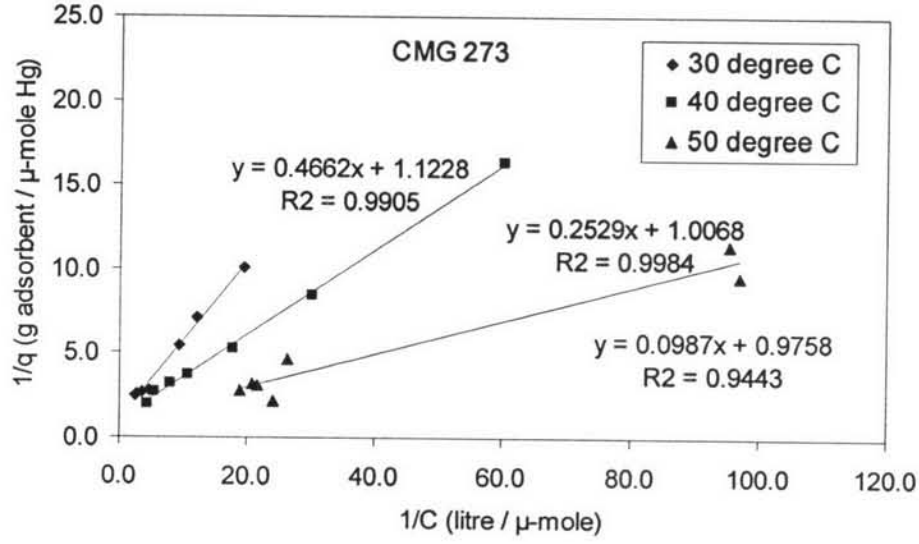

(c)

Figure 4.8 Fitting of experimental data into Langmuir model and determination of Langmuir Isotherm's coefficients for zeolite (a) X, (b) Y, and (c) CMG 273.

From the slope and intercept of Figure 4.8, q_{max} and b can be calculated using equqtion 4.4 and are shown in Table 4.2 below:

Table 4.2 Physical parameters for Langmuir Isotherm of zeolites X, Y and CMG273.

Adsorbent	Temp. (degree C)	q_{max} (μmole/g)	b
X	30	0.12	1.99
	40	0.11	1.24
	50	0.09	0.92
Y	30	0.12	1.97
	40	0.11	1.0
	50	0.09	0.97
CMG273	30	0.89	2.40
	40	0.99	3.98
	50	1.02	9.88

The maximum capacity for zeolites X and Y is quite low compared to CMG273. The adsorption capacity and equilibrium rate constant decreased with increased temperatures which indicates phenomena of physical adsorption while the adsorption capacity and equilibrium rate constant reached its maximum at higher temperature for CMG273 which indicates phenomena of chemisorption due to the presence of impregnated compound (CuS on alumina).

The validity of data shown in Table 4.2 was further checked through fitting of those data into Langmuir Model (equation 4.4) and, then, was compared with experimental data. There is a good agreement between the experimental results and the one site Langmuir model as seen in Figure 4.9.

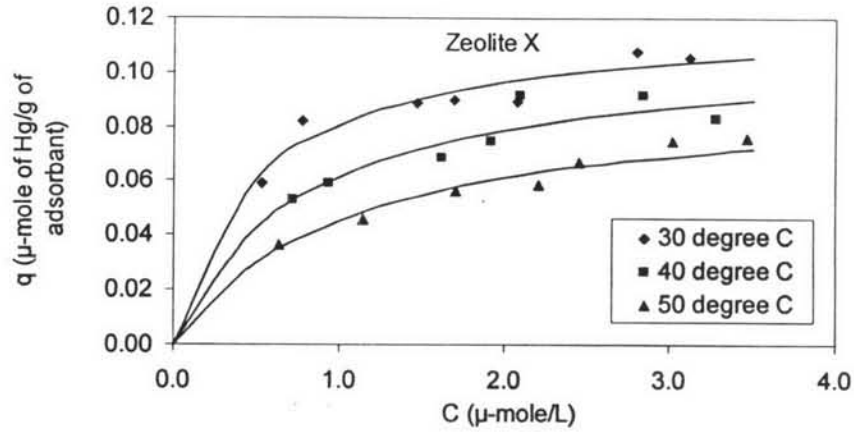

(a)

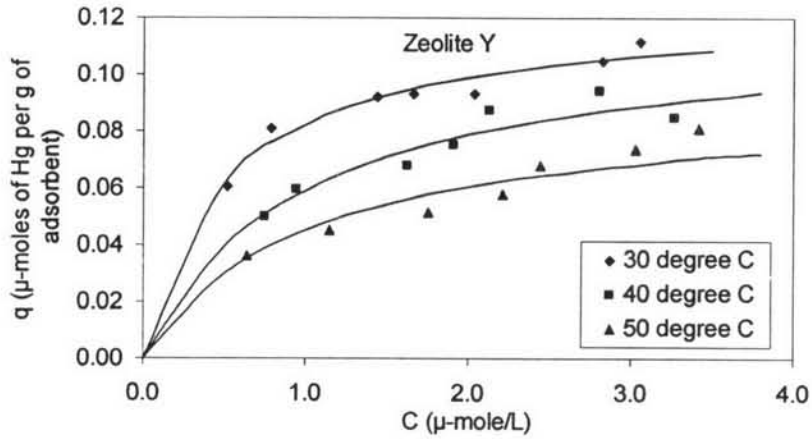

(b)

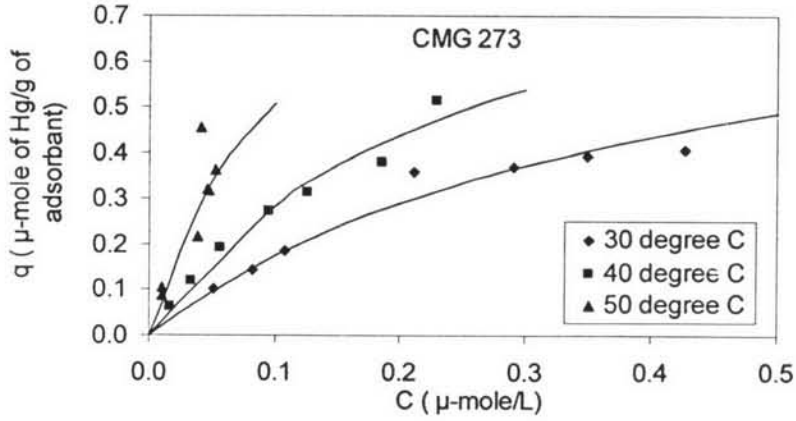

(c)

Figure 4.9 Comparison between experimental results and the one site Langmuir model for zeolites (a) X, (b) Y and (c) CMG273.

4.5 Mathematical Analysis

The basic mass transfer resistances during an adsorption phenomena are explained in Figure 2.4. The different mass transfer resistance govern overall mass transfer resistances. Several studies have shown the determination of overall mass transfer coefficient in which all the individual mass transfer resistance can be lumped together into a single overall mass transfer coefficient as explained in section 2.4.2 (Miyabe, *et al.,* 2000; Brosillon, *et al.,* 2001). The advantage of the method is, that, whole problem can be resolved into the determination of single overall mass transfer coefficient. There is, however, problem with it, that, the determination of overall mass transfer coefficient is strongly based on correlations which are applicable in certain experimental conditions. And, hence, sometimes may fall far from reality.

However, based on experimental results, individual mass transfer resistance can be determined. The overall mass transfer resistance can be determined by slowest mechanism and, thus, can avoid rigorous analysis of correlations. For a uni-porous adsorbent, the problem can be solved via analysis of, mainly, external mass resistance, internal mass resistance and the rate of adsorption/reaction as follows:

4.5.1 External Mass Transfer Resistance

External mass transfer resistance is governed by molecular diffusion of solute into the boundary layer formed due to solid-liquid interaction while the internal mass transfer, which is measure of pore diffusion, depends on internal geometry of adsorbent particle. So, it is necessary to calculate diffusion parameters. The molecular diffusivity of solute A into liquid B can be calculated as follows (Bird, R. R. *et al.*,):

$$D_m = 7.4 \times 10^{-8} \frac{\sqrt{\psi_B M_B T}}{\mu V_A^{0.6}} \qquad (4.1)$$

where T is temperature (in K), ψ_B is association parameter (1.0 for heptane), M_B is molecular weight of B, V is molar volume of solute A (in cm^3/g-mole), and μ is

viscosity of solution (in centi-poise). Table 4.3 shows molecular diffusivity for an average pore opening of 7.4A°;

Table 4.3 Theoretical values of molecular diffusivity of Hg° at 30°C, 40°C and 50°C

	30°C	40°C	50°C
D_m (cm^2/sec)	$2.35*10^{-6}$	$2.6*10^{-6}$	$2.8*10^{-6}$

The lower value of D_m indicates the limitation of external mass resistance and for a non-isothermal behavior of adsorbent particle, the relative importance of internal and external mass transfer can be explained by Biot number. The Biot number for mass transfer, which measures the ratio of internal to external gradients, is defined as:

$$\mathrm{Bi} = \left(\frac{k_f R_P}{3\varepsilon_P D_P}\right) = \frac{Sh}{6}\frac{D_m}{\varepsilon_P D_P} = \frac{Sh}{6}\frac{\tau}{\varepsilon_P} \tag{4.2}$$

where ε_P is porosity of adsorbent particle (Appendix E) and Sh is Sherwood number (ratio of convective to molecular diffusion), defined as:

$$Sh = 2 + 1.1\mathrm{Re}^{0.6} Sc^{0.33} \tag{4.3}$$

where Sc is Schmidt number (ratio of momentum to molecular diffusivity), defined as:

$$Sc = \frac{\mu}{\rho D_m} \tag{4.4}$$

After doing all the calculations Biot number was found to be 3.5 which indicates that in all experimental conditions internal mass transfer resistance is 3.5

times higher than external mass transfer. So, internal mass resistance or surface adsorption can explain overall rate.

4.5.2 Internal Mass Transfer Resistance

Ruthven D.M (1984) has shown that the kinetics of adsorption can be resumed by the following expression:

$$\frac{q_t}{q_\infty} = 2\left(\frac{A}{V}\right)\left(\frac{D_c t}{\pi}\right)^{1/2} \tag{4.5}$$

where A/V is the ratio of external area to particle volume, D_c is the intercrystalline diffusivity and q (q_t, q_{∞}) is mass adsorbed (at time t and at $t \rightarrow \infty$). Under the assumption of constant intercrystalline diffusivity, above relation can be written as (Singh *et al.*, 2004):

$$q_t = K_P . t^{1/2} \tag{4.6}$$

Figure 4.10 shows fitting of experimental data (batch) into equation 4.6.

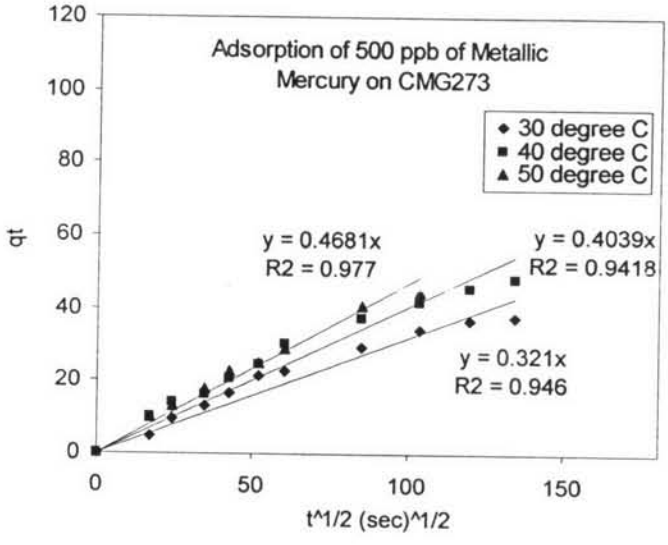

(a)

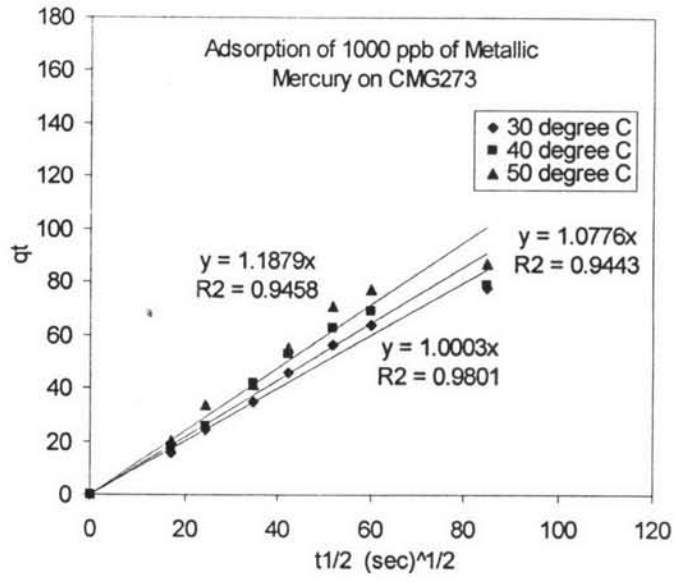

(b)

Figure 4.10 Determination of internal mass resistance for (1) 500 ppb and (2) 1000 ppb of metallic mercury at 30°C, 40°C and 50°C for CMG273.

In Figure 4.10, straight line passing through origin indicates internal mass transfer resistance for CMG273 while no trend was observed in case of zeolites X and Y indicats that surface adsorption may be a rate limiting step for zeolites X and Y which also makes sense based on earlier discussion showing incompatibility between metal mercury and zeolites X and Y.

The different values of k_P (intraparticle diffusion coefficient) were determined from the slop of lines in Figure 4.10 and are listed in Table 4.4 as below:

Table 4.4 K_P values for CMG273 calculated from pore diffusion model

	(Kp in micro-g of Hg/g of adsorant.(min)1/2		
	30°C	40°C	50°C
High Conc.	1.00	1.07	1.18
Low Conc.	0.32	0.40	0.46

Singh *et al.,* (2004) studied intraparticle diffusion coefficient for As^{+3} on alumina at 25°C and reported Kp values as:

- 0.9 (for 0.5 mg/L of As(III) on alumina)
- 2.7 (for 1.5 mg/L of As(III) on alumina)

The values obtained for CMG273 from pore diffusion model are close enough in order of magnitude with their work.

4.5.3 Surface Adsorption

The first order rate kinetics for zeolites X and Y can be written as follows (Singh *et al.,* 2004):

$$\log(q_e - q_t) = \log(q_e) - \left(\frac{k_{ad}}{2.303} \right) t \qquad (4.7)$$

A plot between $\log(q_e - q_t)$ vs t, obtained from the fitting of experimental data (Appendix A1 and A2) into equation 4.7, is shown below which indicates removal of metallic mercury on zeolites X and Y follow first order rate kinetics.

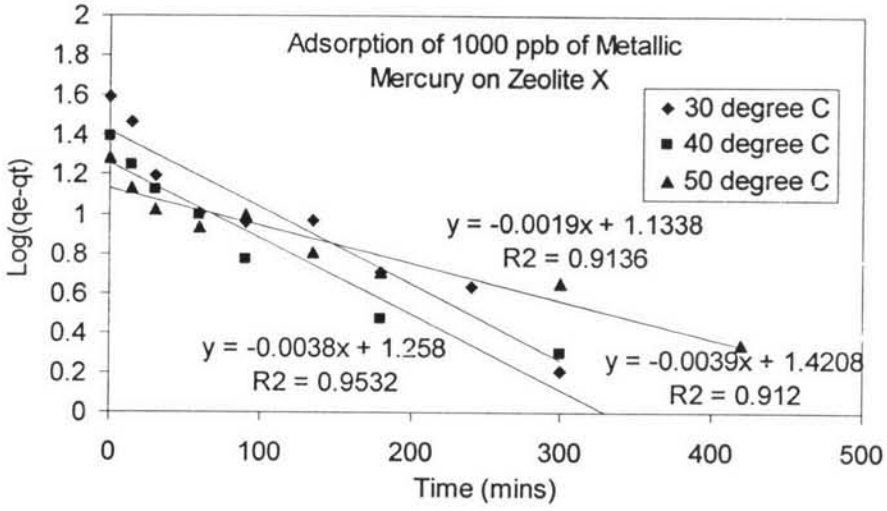

(a)

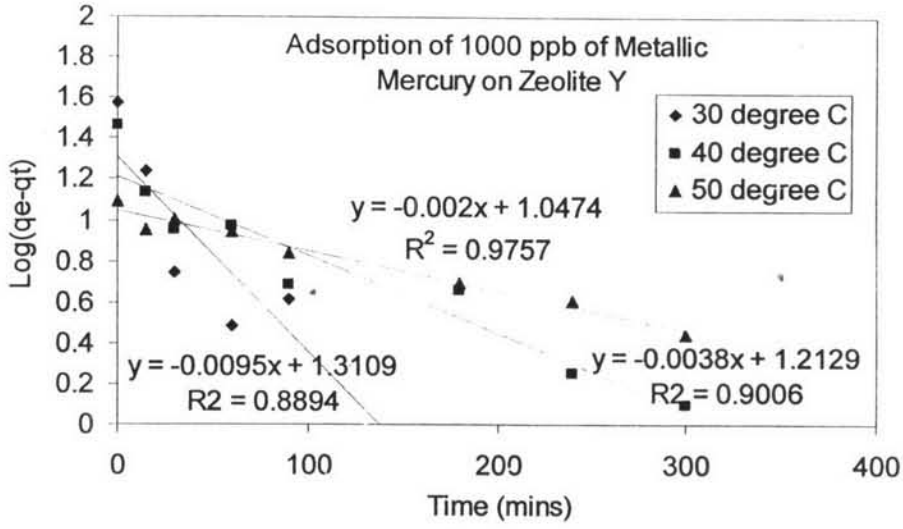

(b)

Figure 4.11 First order rate kinetics of 1000 ppb of metallic mercury for (a) zeolite X and for (b) Y at 30°C, 40°C and 50°C.

4.6 Continuous System

The performance of CMG273 for n-heptane solution containing 800 ppb of metallic mercury was tested in a pilot plant. Since the experiments were limited by time, only 30% of the breakthrough curve is presented in Figure 5.12, Appendix C4.1).

In general, the breakthrough time is set at 0.05 of the ratio of the effluent concentration to the initial concentration, C/C_o. For CMG 273 it was found that the breakthrough time is 20 hrs. A maximum of 95% removal efficiency was achieved. However, in order to reduce the time of test, very low loading (1.0 ml or 0.5 gram) of catalyst could be used, but this would cause some bypasses of mercury making higher outlet concentrations. One could avoid the bypasses and improve the efficiency up to 99.9 % by using higher bed height and amount. By doing so, time of test would also be increased which can be reduced again by using higher feed velocities and concentrations. As n-heptane has very limited solubility of mercury, so, use of solvents having higher solubility of metallic mercury would be better.

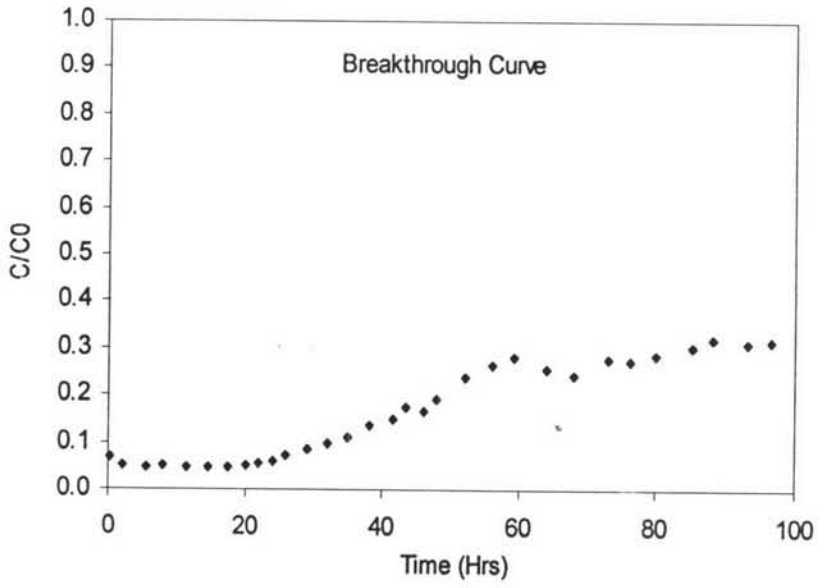

Figure 4.12 Study of continuous system for CMG273, plotting the ratio of the effluent concentration of metallic mercury, C, to intial concentration, C_o (800 ppb), versus time in continues system tested in unit U844.